ASTRONOMY & ASTROPHYSICS
SUPPLEMENT SERIES

Astron. Astrophys. Suppl. Ser. **127,** 101-105 (1998)

Penetrating the "zone of avoidance"⋆,⋆⋆

V. An optical survey for hidden galaxies in the region $90^\circ \leq \ell \leq 110^\circ$, $-10^\circ \leq b \leq +10^\circ$

R. Seeberger and W. Saurer

Institut für Astronomie der Leopold-Franzens-Universität Innsbruck, Technikerstraße 25, A–6020 Innsbruck, Austria

Received March 28; accepted April 21, 1997

Abstract. As the fifth part in our series of papers on galaxies in the "zone of avoidance" (ZOA) of the Milky Way we present 1346 new galaxy candidates discovered during a systematic search on Palomar Observatory Sky Survey (POSS I-E) red-sensitive prints. The region searched comprises 400 square degrees at $90^\circ \leq \ell \leq 110^\circ$, $-10^\circ \leq b \leq +10^\circ$. We list galactic and equatorial coordinates, maximum optical diameters and diameters of the core, if visible, both for the red- and blue-sensitive POSS prints. An asymmetric distribution of the galaxies with respect to the galactic equator is found and can most probably be attributed to the galactic warp.

We also present radial velocities for 14 galaxies measured for the first time which are located in the region where a branch of the Pisces Perseus Supercluster is approaching the ZOA from the south ($\ell \approx 90^\circ$, $b \approx -10^\circ$).

Key words: catalogs — (*ISM*): dust, extinction — galaxies: general — large scale structure of the Universe

1. Introduction

The significance of investigating the extragalactic sky in the "zone of avoidance" (ZOA) of the Galaxy, our search methods, and the material used for our survey (red sensitive POSS I-E prints) has been described and discussed in detail in previous parts of our series (Saurer et al. 1997 (part IV); Lercher et al. 1996 (part III); Seeberger et al. 1996 (part II), and Weinberger et al. 1995 (part I)).

A graphical overview of the status of our survey is shown in Fig. 1. Not included in this figure is the recently started survey in the area around the Circinus Galaxy at $306^\circ \leq \ell \leq 316^\circ$, $-5^\circ \leq b \leq +5^\circ$.

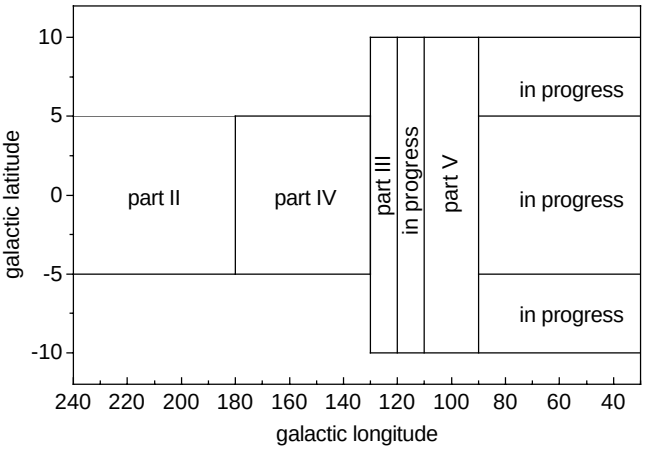

Fig. 1. The status of the Innsbruck-survey for optical galaxies in the ZOA. The references for the various parts can be found in the text

In this paper we present the results of our survey within the area $90^\circ \leq \ell \leq 110^\circ$, $-10^\circ \leq b \leq +10^\circ$. This region is of special interest also because a branch of the Pisces-Perseus-Supercluster (PPScl) starting at (ℓ, b) $\approx$ (120°, -30°) and extending to the north is approaching the ZOA at $\ell \approx 90^\circ$, coming from the south (see, e.g., Focardi et al. 1984; Merighi et al. 1986; Meurs & Harmon 1988). Seeberger et al. (1994) could pursue this branch of the PPScl to $b \approx -5^\circ$. Mainly in the light of new doubt about the crossing of the main ridge of the PPScl (at $\ell \approx 160^\circ$) through the ZOA which was brought into discussion by Lu & Freudling (1995) it would be interesting to study this feature in more detail. For this purpose we have started to carry out radial velocity measurements by

Send offprint requests to: Walter.Saurer@uibk.ac.at

⋆ Partly based on observations collected at the Observatoire de Haute-Provence (OHP), CNRS, France.

⋆⋆ Table 2 is only available in electronic form at the CDS via anonymous ftp to cdsarc.u-strasbg.fr (130.79.128.5) or via http://cdsweb.u-strasbg.fr/Abstract.html

means of low resolution spectroscopy on a selected sample of galaxies at the southern and northern parts of the ZOA within this region.

2. Observations

Low resolution spectral observations were carried out in August 1992 with the CARELEC spectrograph attached to the 1.92 m telescope of the Observatoire de Haute Provence (OHP). The resolution chosen was 260 Å/mm, the slit-width 2.″2. The detector used was a Tektronix CCD chip with 512×512 pixels. The wavelength range covered is 3730−7100 Å with a scale of ≈ 7 Å per pixel and a spectral resolution of ≈ 14 Å (FWHM). The wavelength calibration was done by means of a He-laboratory lamp and Hiltner 102 served as a standard star. The data reduction was carried out with the software package MIDAS.

3. Results and discussion

Figure 2 shows a grey scale map of the 60 μ flux densities taken from the IRAS Sky Survey Atlas (Wheelock et al. 1991), using the software provided by Sky View (http://skview.gsfc.nasa.gov/skyview.html). Also shown in this figure is the distribution of our 1346 new galaxy candidates. As can be seen, similar to the results in our previous work, the IRAS 60 μ flux densities can serve as a rough indicator for galactic extinction also in this region. A result which is confirmed in a more elaborate way by Gajdošík & Weinberger (1997). The 60 μ flux density distribution seems to account for the overall distribution of the galaxies.

The most striking feature in Fig. 2 is the pronounced asymmetry both in the distribution of the galaxies and in the IRAS 60 μ flux densities. There are 1136 galaxies located to the south of the galactic equator, whereas only 15.6% of all galaxies can be found in the northern part. An investigation of the diameters leads to the result that the southern galaxies, on average, exhibit larger projected sizes. This gives us further evidence that the asymmetry in distribution might be caused by a south-north extinction gradient within our galaxy (see Cameron 1990). The observed asymmetry is most probably caused by the galactic warp which is expected to exhibit a maximum north to the galactic plane at $\ell \approx 90°$ (Henderson et al. 1982; Miyamoto et al. 1988; Djorgovski & Sosin 1989; Freudenreich et al. 1994).

An additional and interesting feature is located in the region studied here. A branch of the PPScl is approaching the ZOA at $90° \leq \ell \leq 95°$, $b \approx -10°$ from the south. By means of 21 cm measurements Seeberger et al. (1994) have traced this branch until $b \approx -5°$. If this feature penetrates deeper into the ZOA, its further route cannot be estimated from our galaxy distribution. It might remain straight to the north-west (with respect to the galactic coordinates) within the ZOA. In this case it would, if it

Table 1. Heliocentric velocities of a sample of galaxies. Given are the names, the galactic longitudes and latitudes, the heliocentric velocities as a result from this work and values found in the literature. The last column gives the number of absorption/emission lines used for determining the velocity for each galaxy

name	ℓ	b	v_{hel} this	v_{hel} ref other	# of lines
MCG+08−36−010	81.64	9.47	8004	8081 ST92	7
CGCG 493−2	82.07	−15.08	7502		17
UGC 11507	83.70	9.71	6800		2
MCG+08−36−016	83.93	9.67	6900	7071 SA76	6
UGC 11775	83.94	−12.31	4426	4828 KA88	10
UGC 11772	83.95	−12.24	4494	4451 KA88	10
UGC 11781	84.31	−12.18	4317	4774 KA88	9
CGCG 257−36	85.57	9.62	7260		8
UGC 11757	87.70	−6.88	4234	4523 BO93	12
				4351 HA91	
MCG+06−47−007	87.75	−11.44	5221		11
UGC 11892	88.82	−15.55	5812	5638 WE93	9
UGC 11893	88.84	−15.36	5432	5564 WE93	7
UGC 11801	90.64	−7.25	3925		10
UGC 11798	90.64	−7.23	3841	3984 BO93	7
				4029 HA91	
				4031 SE94	
UGC 11797	90.64	−7.23	4214	4043 SE94	9
				5572 SE94	
G092.15−02.28	92.15	−2.28	3556		7
G092.17−02.29	92.17	−2.29	3727	3775 KE87	7
UGC 11800	92.42	−5.19	5335	5520 BO93	10
UGC 11805	92.52	−5.26	5455	5679 SE94	11
UGC 11804	92.52	−5.27	5645	5440 DA95	12
UGC 11911	94.47	−9.31	5018	5996 MA86	10
UGC 11997	97.27	−9.78	4508		9
UGC 11874	98.02	−2.84	656		9
UGC 12096	101.67	−6.97	10514		7
UGC 12095	101.67	−6.97	412		5
UGC 12089	101.74	−6.73	9446		10
UGC 12091	101.74	−6.73	9688		7
UGC 12223	103.83	−8.95	5330		10
G105.42+09.58	105.42	9.58	8226	8411 SE94	5
G109.75−08.40	109.75	−8.40	10291		9

References to the table:
BO93: Botinelli et al. (1993)
DA95: Davoust & Considère (1995)
HA91: Haynes & Giovanelli (1991)
KA88: Karachentseva et al. (1988)
KE87: Kerr & Henning (1987)
MA86: Mazarella & Balzano (1986)
SA76: Sandage (1976)
SE94: Seeberger et al. (1994)
ST92: Strauss et al. (1992)
WE93: Wegner et al. (1993).

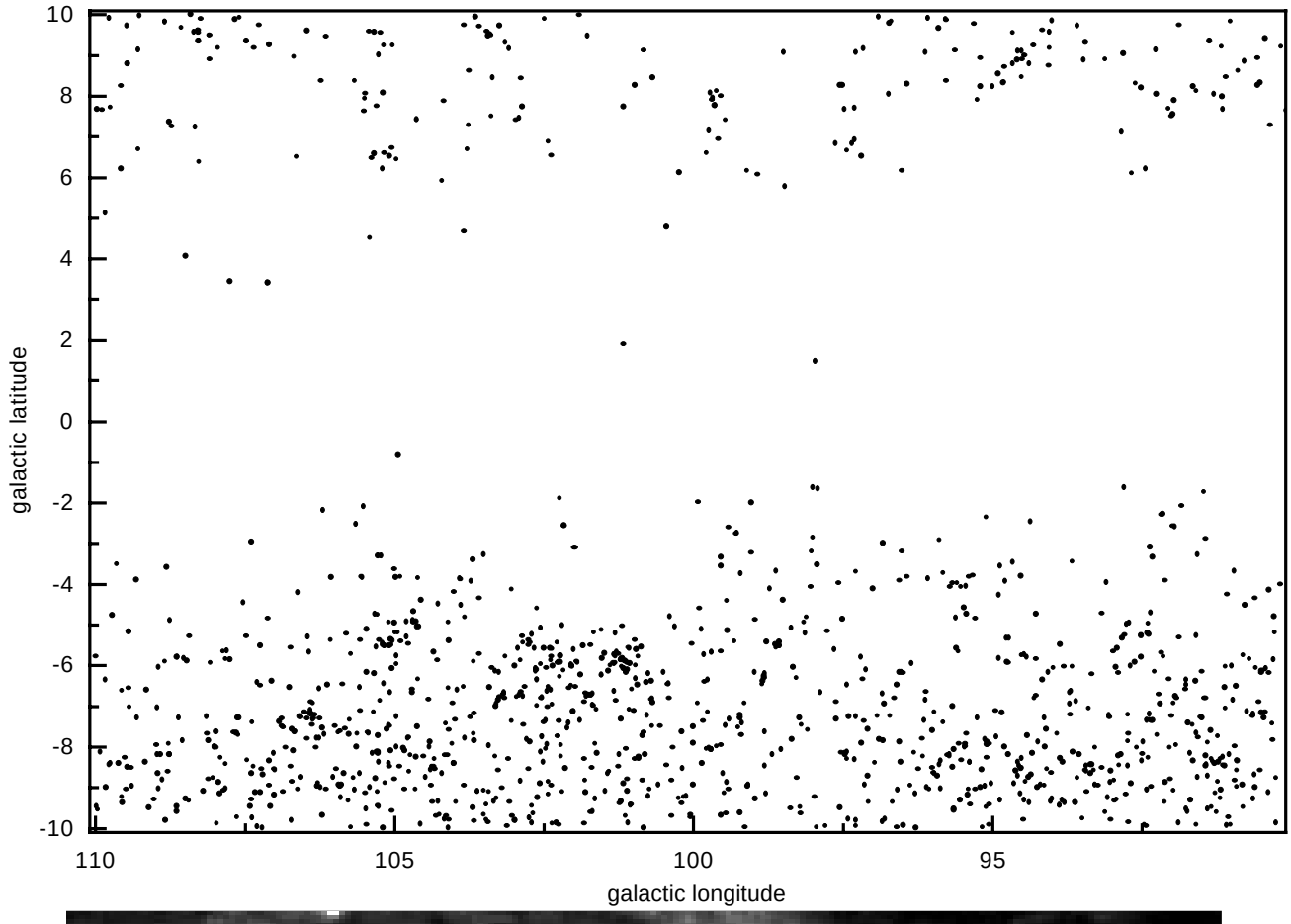

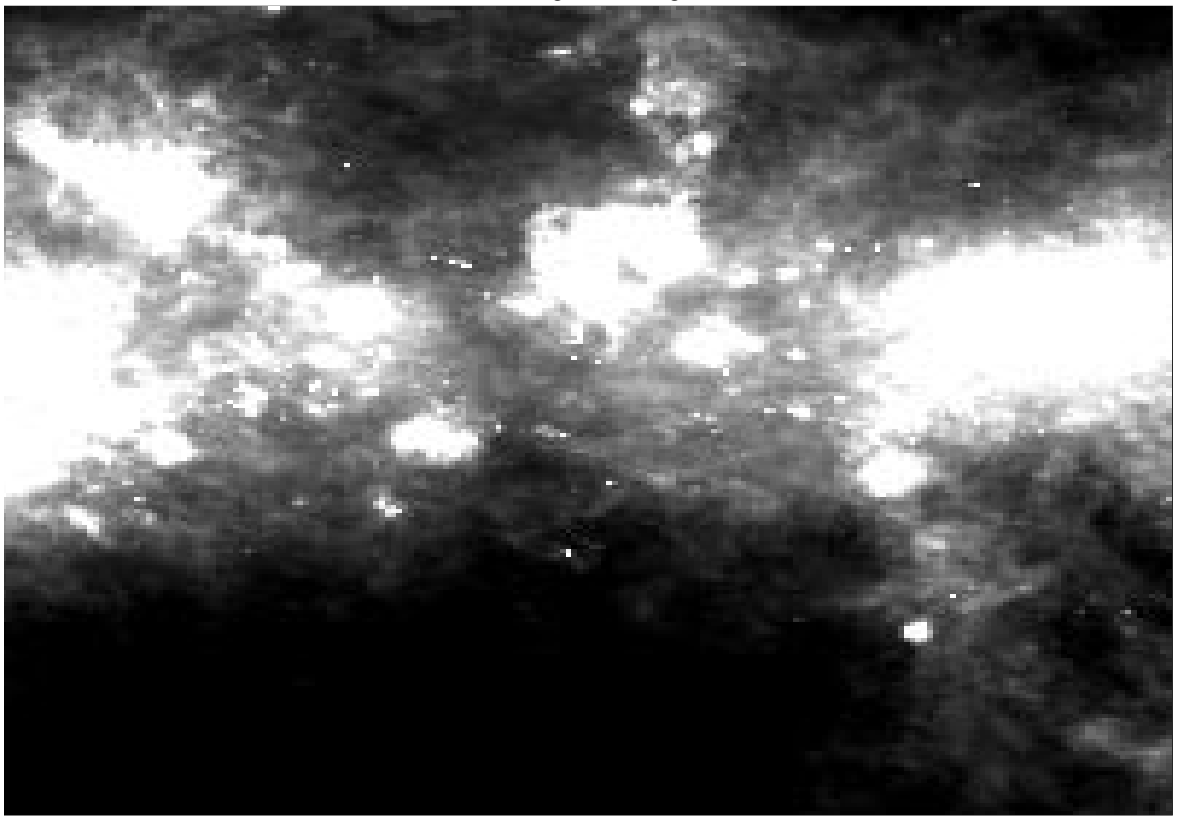

Fig. 2. Top: distribution of the new galaxies in the region $90^\circ \leq \ell \leq 110^\circ$, $-10^\circ \leq b \leq +10^\circ$ in galactic coordinates. Bottom: the 60 μ flux density taken from the IRAS Sky Survey Atlas; black (white) areas correspond to low (high) flux densities. Both parts of the figure represent the same region

really penetrates the ZOA, best be recovered at $\ell \approx 80°$, $b \approx +10°$. To investigate this feature we have selected a sample of galaxies at the northern and southern parts of the ZOA and measured their radial velocities. To determine the velocities we have used absorption lines and, where available, lines which appear in emission. The errors of these measurements are estimated to be less than $\approx 200\,\mathrm{km/s}$.

The names and coordinates of these galaxies, mainly chosen at the southern part of the ZOA, together with our results are listed in Table 1. For the literature search we have made use of the Simbad database and the NASA/IPAC Extragalactic Data-base (NED). For 14 galaxies Table 1 gives heliocentric radial velocities measured for the first time, according to these databases.

Galaxies of the PPScl typically exhibit velocities of $\approx 5000\,\mathrm{km/s}$ (see, e.g., Haynes & Giovanelli 1986). An inspection of Table 1 shows, that galaxies of our sample only in the southern region ($b \approx -10°$) fit this condition, say within an error-range of $\pm 1000\,\mathrm{km/s}$, and can thus be regarded as possible members of the PPScl. Unfortunately, in the northern part ($b \approx +10°$) only very few galaxies (5) could be measured until now. However, all of these have velocities well above $5000\,\mathrm{km/s}$.

Finally, in Table 2 our 1346 optical galaxy candidates are presented in detail. The whole compilation is available from the Simbad database. The first column gives the name of the galaxy. If the name is followed by a colon, the classification as a galaxy is less certain. Columns 2 and 3 (4 and 5) list the right ascension and declination 1950.0 (2000.0). Column 6 gives the designation of the POSS prints on which the object was found, and Cols. 7 and 8 the location of the object (x, y) in cm. In Cols. 9 and 10 (11 and 12) the maximum diameter of the galaxy candidate and, if visible, the diameter of the core on POSS I-E (POSS I-O (blue-sensitive)) can be found. All diameters are in arcmin. The last column gives cross-identifications. If we have found an IRAS point source within $1'$ of radius around the object, the IRAS name was included in this column. If the IRAS name is followed by an asterisk, more than one galaxy candidate coincides with the position of this IRAS source.

As pointed out in our previous papers only a few percent of the optical galaxies turned out to have counterparts in the IRAS Point Source Catalogue. The size distribution function again indicates a complete size limited sample down to a diameter limit of $\approx 0\farcm4$.

Acknowledgements. We would like to thank Prof. R. Weinberger for his help and fruitful discussions. This work was supported by the "Fonds zur Förderung der wissenschaftlichen Forschung", project No. P 8325-PHY and by the "Jubiläumsfonds der Österreichischen Nationalbank", project No. 4713 (computer facilities). This research has made use of the NASA/IPAC Extragalactic Data-base (NED) which is operated by Jet Propulsion Laboratory, California Institute of Technology, under contract with the National Aeronautics and Space Administration; and of the Simbad database, operated at CDS, Strasbourg, France.

References

Botinelli L., Durand N., Fouqué P., et al., 1993, A&AS 102, 57
Cameron L.M., 1990, A&A 233, 16
Davoust E., Considère S., 1995, A&AS 110, 19
Djorgovski S., Sosin C., 1989, ApJ 341, L13
Focardi P., Marano B., Vettolani G., 1984, A&A 136, 178
Freudenreich H.T., Berriman G.B., Dwek E., et al., 1994, ApJ 429, L69
Gajdošík M., Weinberger R., 1997, A&A (in press)
Haynes M.P., Giovanelli R., 1986, ApJ 306, L55
Haynes M.P., Giovanelli R., 1991, ApJS 77, 331
Henderson A.P., Jackson P.D., Kerr F.J., 1982, ApJ 263, 116
Karachentseva V.E., Karachentseva I.D., Lebedev V.S., 1988, Astrofizik. Issledovanija 26, 42
Kerr F.J., Henning P.A., 1987, ApJ 320, L99
Lercher G., Kerber F., Weinberger R., 1996, A&AS 117, 369
Lu N.Y., Freudling W., 1995, ApJ 449, 527
Mazarella J.M., Balzano V.A., 1986, ApJS 62, 751
Merighi R., Focardi P., Marano B., Vettolani G., 1986, A&A 160, 398
Meurs E.J.A., Harmon R.T., 1988, A&A 206, 53
Miyamoto M., Yoshizawa M., Suzuki S., 1988, A&A 194, 107
Sandage A., 1976, PASP 88, 367
Saurer W., Seeberger R., Weinberger R., 1997, A&A (in press)
Seeberger R, Huchtmeier W.K., Weinberger R., 1994, A&A 286, 17
Seeberger R., Saurer W., Weinberger R., 1996, A&AS 117, 1
Strauss M.A., Huchra J.P., Davis M., et al., 1992, ApJS 83, 29
Wegner G., Haynes M.P., Giovanelli R., 1993, AJ 105, 1251
Weinberger R., Saurer W., Seeberger R., 1995, A&AS 110, 269
Wheelock S., Gautier T.N., Chillemi J., et al., 1991, IRAS Sky Survey Atlas Explanatory Supplement

Table 2. Optically detected galaxies in the region $90° \leq \ell \leq 110°$, $|b| \leq 10°$

ZOAG G	α(B1950.0)	δ(B1950.0)	α(J2000.0)	δ(J2000.0)	POSS	x(mm)	y(mm)	$\mathcal{D}'E$	$\mathcal{D}'E_C$	$\mathcal{D}'O$	$\mathcal{D}'O_C$	cross id.
090.00−9.53	21 46 58	41 09.5	21 49 00	41 23.5	806	37.0	110.2	0.20		0.30		
090.01−9.29	21 46 11	41 21.0	21 48 12	41 35.0	806	45.1	120.5	0.20		0.15		
090.06−9.52 :	21 47 09	41 12.4	21 49 11	41 26.4	806	35.5	112.8	0.20		0.15		
090.08+7.65 :	20 33 41	53 07.2	20 35 05	53 17.6	543	48.6	112.8	0.10		0.10		
090.17+9.21 :	20 25 30	54 06.2	20 26 49	54 16.1	543	115.7	161.9	0.10		0.10		
090.18−4.01	21 27 34	45 24.3	21 29 26	45 37.5	589	247.8	14.7	0.25		0.25	0.05	IRAS 21275+4524
090.26−8.77	21 45 23	41 54.1	21 47 24	42 08.0	806	54.1	149.5	0.30		0.30		
090.26−9.87	21 49 09	41 03.4	21 51 11	41 17.5	806	14.5	106.1	0.15		0.15		
090.28−5.19	21 32 31	44 36.2	21 34 25	44 49.6	806	183.0	291.0	0.65		0.55		
090.29−4.79	21 31 01	44 54.2	21 32 55	45 07.5	806	197.0	307.2	0.30		0.30		
090.30−5.86	21 35 06	44 07.7	21 37 02	44 21.2	806	158.2	265.9	0.25	0.10	0.20	0.05	
090.31−7.83	21 42 18	42 39.1	21 44 17	42 52.9	806	86.1	188.8	0.15		0.15		
090.32−7.42	21 40 51	42 58.1	21 42 49	43 11.9	806	100.7	205.0	0.45	0.10	0.40	0.15	
090.35+7.28 :	20 36 44	53 06.7	20 38 09	53 17.3	598	334.6	110.7	0.15		0.10		
090.38−4.15	21 28 56	45 26.1	21 30 48	45 39.3	589	234.3	15.7	0.40		0.30	0.20	
090.38−6.18	21 36 38	43 56.1	21 38 34	44 09.7	806	143.2	255.8	0.25		0.25		
090.39−9.12	21 47 09	41 43.0	21 49 10	41 57.0	580	341.8	133.9	0.80		0.80		UGC 11819
090.43−6.07	21 36 23	44 03.2	21 38 19	44 16.8	806	145.5	262.0	0.20	0.10	0.15		
090.44−7.15	21 40 24	43 14.6	21 42 22	43 28.3	806	105.7	219.8	0.50	0.10	0.40	0.05	
090.44+9.42	20 25 22	54 26.4	20 26 40	54 36.3	543	117.4	179.8	0.10		0.10		
090.46−7.29 :	21 41 00	43 09.3	21 42 58	43 23.1	806	99.7	215.0	0.10		0.10		
090.47−6.12	21 36 46	44 02.3	21 38 42	44 15.9	806	142.0	261.2	0.45		0.35		
090.50−6.13	21 36 55	44 03.5	21 38 51	44 17.1	806	140.5	262.4	0.25	0.10	0.10	0.05	
090.50−6.18	21 37 07	44 00.8	21 39 03	44 14.4	806	138.7	260.0	0.80		0.70	0.25	
090.50−7.16	21 40 41	43 17.2	21 42 39	43 30.9	806	103.0	222.1	0.50	0.30	0.40		IRAS 21406+4317
090.52−8.57	21 45 46	42 13.1	21 47 46	42 27.1	806	51.3	166.5	0.20	0.10	0.20		
090.52+8.33	20 31 46	53 52.4	20 33 08	54 02.7	543	66.5	152.0	0.20		0.10	0.05	
090.54−6.89	21 39 53	43 30.5	21 41 50	43 44.2	806	111.1	233.5	0.40		0.40		
090.57+8.26	20 32 19	53 52.4	20 33 41	54 02.7	543	61.6	152.3	0.10		0.10		
090.57+8.93 :	20 28 34	54 15.7	20 29 54	54 25.8	543	92.7	171.7	0.10		0.05		
090.60−6.06	21 37 04	44 10.3	21 39 00	44 23.9	806	139.1	168.4	0.30	0.10	0.20		
090.61−4.34 :	21 30 38	45 27.3	21 32 31	45 40.6	589	218.4	16.4	0.15		0.20	0.10	
090.61−8.99	21 47 34	41 57.1	21 49 35	42 11.1	806	32.6	153.2	0.20		0.15		
090.62−8.68	21 46 32	42 11.8	21 48 33	42 25.8	806	43.7	165.8	0.15		0.10		
090.64−7.19	21 41 23	43 20.8	21 43 21	43 34.6	806	96.3	225.4	1.00		0.70		UGC 11798
090.64−7.22	21 41 29	43 19.5	21 43 27	43 33.3	806	95.3	224.3	1.30		1.30		UGC 11797
090.64−9.28	21 48 42	41 45.4	21 50 44	41 59.5	580	326.2	135.5	0.45	0.15	0.40	0.10	5ZW 378
090.65−7.24	21 41 36	43 19.2	21 43 34	43 33.0	806	94.2	224.1	0.65		0.60		UGC 11801
090.70−5.84	21 36 42	44 24.3	21 38 38	44 37.9	806	142.9	280.9	0.40	0.15	0.30	0.10	
090.75−7.13	21 41 37	43 27.9	21 43 35	43 41.7	806	94.2	231.8	1.00	0.15	0.90	0.10	UGC 11799, IRAS 21416+4327
090.78−4.51 :	21 31 59	45 26.6	21 33 52	45 40.0	806	187.9	336.4	0.25	0.10	0.10		
090.79+8.85 :	20 29 56	54 23.8	20 31 16	54 34.0	543	81.9	179.2	0.10		0.10		
090.81−5.74	21 36 46	44 32.9	21 38 41	44 46.5	806	142.4	288.5	0.40	0.15	0.20	0.05	
090.81−9.48 :	21 50 04	41 42.3	21 52 06	41 56.4	580	312.8	132.2	0.10		0.00		
090.82−8.93	21 48 14	42 07.9	21 50 15	42 22.0	806	26.5	168.0	0.25	0.10	0.20	0.10	
090.89+8.62	20 31 34	54 20.3	20 32 54	54 30.6	543	68.9	176.5	0.80	0.40	0.60		UGC 11592
090.90−8.34	21 46 31	42 38.3	21 48 31	42 52.3	806	44.5	189.4	0.40		0.30	0.10	
090.91−8.57	21 47 20	42 28.2	21 49 20	42 42.2	806	36.1	180.8	0.45	0.10	0.50	0.25	
090.91−8.98 :	21 48 45	42 09.2	21 50 46	42 23.3	806	21.6	164.5	0.20		0.10		
090.92−8.32	21 46 32	42 40.0	21 48 32	42 54.0	806	44.5	191.0	0.15		0.15		
090.93−6.51	21 40 06	44 02.9	21 42 03	44 16.6	806	109.8	262.5	0.65	0.10	0.50	0.10	
090.95−7.98	21 45 28	42 56.8	21 47 27	43 10.7	806	55.4	205.4	0.25	0.15	0.25	0.10	
090.95−7.99	21 45 31	42 56.3	21 47 30	43 10.2	806	55.3	205.1	0.30	0.10	0.20		
090.95−8.83	21 48 26	42 17.7	21 50 27	42 31.8	580	327.7	164.2	0.25		0.35		
090.96−3.68 :	21 29 31	46 10.8	21 31 22	46 24.1	589	228.3	55.1	0.20	0.10	0.10		
090.98−6.85 :	21 41 34	43 49.8	21 43 31	44 03.6	806	95.1	251.3	0.25		0.05		
091.00−6.01	21 38 36	44 28.4	21 40 32	44 42.1	806	124.9	285.0	0.40	0.10	0.30	0.10	
091.02−9.92	21 52 24	41 29.7	21 54 27	41 43.9	580	289.8	120.1	0.50		0.40		IRAS 21524+4130
091.02+9.83	20 25 15	55 08.6	20 26 31	55 18.5	543	119.3	217.3	0.10		0.10		
091.04−8.18	21 46 31	42 51.0	21 48 31	43 05.0	806	45.0	200.5	0.10		0.10		
091.05−9.72	21 51 52	41 39.8	21 53 54	41 54.0	580	294.8	129.2	0.45		0.45	0.10	
091.07−4.26	21 32 15	45 49.5	21 34 08	46 02.9	589	203.2	35.9	0.25		0.25		
091.08−9.93	21 52 41	41 31.3	21 54 44	41 45.5	580	286.8	121.3	0.30		0.35		
091.09+8.46	20 33 18	54 24.3	20 34 39	54 34.7	543	55.4	180.8	0.15		0.15		
091.11−6.03	21 39 07	44 32.1	21 41 03	44 45.8	806	120.0	288.3	0.20		0.25	0.05	
091.11−7.05 :	21 42 49	43 45.6	21 44 47	43 59.4	806	83.0	248.1	0.10		0.10		
091.12−6.54	21 41 00	44 09.4	21 42 57	44 23.2	806	101.2	268.5	0.50	0.30	0.25		ZW 529.002
091.12−8.47 :	21 47 53	42 40.9	21 49 53	42 54.9	806	31.4	192.4	0.10		0.00		
091.15−8.25	21 47 14	42 52.1	21 49 14	43 06.1	806	38.0	202.2	0.20		0.15		
091.15−8.45 :	21 47 56	42 42.8	21 49 56	42 56.8	806	30.9	194.0	0.15	0.05	0.10		
091.15+7.67 :	20 37 50	53 58.8	20 39 13	54 09.5	543	18.6	160.3	0.10		0.05		
091.16+7.98 :	20 36 12	54 10.8	20 37 34	54 21.4	598	334.7	168.2	0.20		0.10		
091.17+9.22 :	20 29 19	54 54.8	20 30 37	55 05.0	543	88.7	206.2	0.15		0.10		
091.18−9.06	21 50 09	42 15.4	21 52 10	42 29.5	580	310.7	161.7	0.30	0.15	0.30	0.05	
091.19−8.29 :	21 47 33	42 51.5	21 49 33	43 05.5	806	34.9	201.8	0.10		0.10		
091.19−9.26	21 50 54	42 06.8	21 52 56	42 21.0	580	303.7	153.5	0.20		0.20		
091.20−6 65	21 41 46	44 07.2	21 43 43	44 21.0	806	93.8	266.9	0.15		0.10		
091.22−8.37	21 47 57	42 49.5	21 49 57	43 03.5	806	31.1	200.0	0.15		0.10		
091.23−7.74	21 45 46	43 18.7	21 47 45	43 32.7	806	53.5	224.9	0.15		0.15		
091.23−8.86 :	21 49 40	42 26.6	21 51 41	42 40.7	580	315.0	171.7	0.15		0.40		
091.25−9.61 :	21 52 20	41 52.7	21 54 22	42 06.9	580	289.7	140.6	0.10		0.00		
091.27−9.14 :	21 50 50	42 15.3	21 52 51	42 29.5	580	303.8	161.2	0.10		0.00		
091.29−8.40	21 48 20	42 50.1	21 50 20	43 04.2	806	27.4	200.8	0.15		0.10		
091.30+8.05 :	20 36 21	54 19.7	20 37 43	54 30.3	543	31.6	178.2	0.10		0.00		
091.32−8.36	21 48 20	42 53.5	21 50 20	43 07.6	806	27.4	203.9	0.25		0.20		